

J/Ψ Production in pp Collisions at $\sqrt{s} = 200$ GeV at RHIC

Fred Cooper,^{1,*} Ming X. Liu,^{2,†} and Gouranga C. Nayak^{3,‡}

¹ *National Science Foundation, Arlington,*

VA 22230, USA and T-8, Theoretical Division,

Los Alamos National Laboratory, Los Alamos, NM 87545, USA

² *P-25, Physics Division, Los Alamos National Laboratory, Los Alamos, NM 87545, USA*

³ *C. N. Yang Institute for Theoretical Physics,*

Stony Brook University, SUNY, Stony Brook, NY 11794-3840, USA

(Dated: October 17, 2018)

Abstract

We study J/ψ production in pp collisions at RHIC within the PHENIX detector acceptance range using the color singlet and color octet mechanism which are based on pQCD and NRQCD. Here we show that the color octet mechanism reproduces the RHIC data for J/ψ production in pp collisions with respect to the p_T distribution, the rapidity distribution and the total cross section at $\sqrt{s} = 200$ GeV. The color singlet mechanism leads to a relatively small contribution to the total cross section when compared to the octet contribution.

PACS numbers:

arXiv:hep-ph/0402219v2 7 Sep 2004

Understanding the J/ψ production mechanism in high energy hadronic collisions is an important topic in QCD and in collider physics. Two prominent mechanisms for J/ψ production at high energy colliders are 1) the color singlet mechanism [1, 2] and 2) the color octet mechanism [3], both of which rely on pQCD and NRQCD. At Tevatron energies, the color singlet mechanism was found to give too small a yield and the color octet mechanism for J/ψ production was then introduced [4, 5]. It was shown that the color octet mechanism, with both parton fusion and parton fragmentation processes included, reproduced the Tevatron data [6]. The relativistic heavy ion collider (RHIC) at Brookhaven is a unique facility which can collide unpolarized and polarized protons at $\sqrt{s} = 200$ and 500 GeV as well as two heavy nuclei such as gold on gold. It has also the capability of exploring light-heavy interactions such as the collisions pAu and dAu at $\sqrt{s} = 200$ GeV. The unpolarized pp collision data serve as a baseline for understanding collective phenomena such as the production of a quark gluon plasma that is expected in the heavy ion collisions as well as providing the necessary information needed to extract interference terms generated when considering polarized pp collisions. One of the key things to be measured in Au Au collisions as well as in polarized pp collision is J/ψ production. In relativistic heavy ion collisions, J/ψ suppression has been posited to be one of the major signatures of the production of the quark-gluon plasma [7]. In case of polarized pp collisions the measurement of J/ψ production is an important ingredient in extracting the polarized gluon distribution function for the proton directly. For that reason, understanding the dominant mechanism of J/ψ production is important. Thus it is crucial to first determine the relative importance of color singlet and color octet contributions in the existing unpolarized proton-proton scattering data at RHIC energies. In this paper we will study J/ψ production in pp collisions at RHIC by using the color singlet and color octet mechanism within pQCD and NRQCD. We will study the p_T distribution, rapidity distribution and total cross section of the J/ψ production at $\sqrt{s} = 200$ GeV pp collisions and compare those with the recent measurements by the PHENIX collaboration at RHIC [8].

In the color singlet mechanism, quarkonium is formed as a non relativistic bound state of a heavy quark-antiquark pair via static gluon exchange. In this mechanism it is assumed that the $Q\bar{Q}$ pair is produced in the color singlet state at the production point with appropriate spin (S) and orbital angular momentum quantum number (L) and then evolves into a bound state ${}^{2S+1}L_J$ with total angular momentum quantum number (J). The relative momentum

of the $Q\bar{Q}$ pair inside the quarkonium is assumed to be small compared to the mass m of the heavy quark so that the Q and \bar{Q} will not fly apart to form heavy mesons. The non-relativistic non-perturbative wave functions and its derivatives appearing in the color singlet calculation are either determined from the potential model or taken from experiment.

The leading term in the p_T distribution for the cross section for J/ψ production first occurs at order α_s^3 . The p_T distribution for heavy quarkonium production in the color singlet mechanism is given by:

$$\begin{aligned} \frac{d\sigma}{dp_T}(AB \rightarrow J/\psi, \chi_J + X) &= \sum_{a,b} \int dy \int dx_a x_a \\ & f_{a/A}(x_a, Q^2) x'_b f_{b/B}(x'_b, Q^2) \frac{2p_T}{x_i - \frac{M_T}{\sqrt{s}} e^y} \\ & \frac{d\hat{\sigma}}{d\hat{t}}(ab \rightarrow ({}^{2S+1}L_J)c), \end{aligned} \quad (1)$$

where

$$x'_b = \frac{1}{\sqrt{s}} \frac{x_b \sqrt{s} M_T e^{-y} - M^2}{x_b \sqrt{s} - M_T e^y}. \quad (2)$$

In the above equation a, b, c are light quarks and gluons. $f(x, Q^2)$ is the parton distribution function at longitudinal momentum fraction x and at factorization scale Q . M is the mass of the bound state quarkonium and $M_T = \sqrt{p_T^2 + M^2}$. The partonic level differential cross section $\frac{d\hat{\sigma}}{d\hat{t}}(ab \rightarrow ({}^{2S+1}L_J)c)$ contain the non-relativistic wave function $|R(0)|^2$ (for direct J/ψ process) and its derivatives $|R'(0)|^2$ (for χ_J processes) at the origin [1]. For the non relativistic wave functions at the origin we take the Buchmuller-Tye wave function [9]. The numerical value is [9]: $|R(0)|^2=0.81 \text{ GeV}^3$. For the derivative of the radial wave function at origin we use [10]: $\frac{9}{2\pi} \frac{|R'(0)|^2}{M^4}=15 \text{ MeV}$.

In the color octet mechanism the relativistic effects are taken into account which are neglected in the color singlet case. In the color octet mechanism using an effective field theory called non-relativistic QCD (NRQCD), the dynamical gluon enters into Fock state decompositions of the quarkonium states. In NRQCD the expansion is carried out in terms of the relative velocity v ($v^2 \sim 0.23$ for $C\bar{C}$ system and 0.1 for $B\bar{B}$ system) of the $Q\bar{Q}$ bound state. The NRQCD Lagrangian density is given by

$$\mathcal{L}_{NRQCD} = \mathcal{L}_{light} + \mathcal{L}_{heavy} + \mathcal{L}_{correction}. \quad (3)$$

In the above equation light refers to light quarks and gluons, heavy refers to lowest order non-relativistic heavy quarks part and correction is higher order corrections in heavy quark

sector. The explicit expressions for the three terms can be found in [4]. In NRQCD the dynamical gluons enter into the Fock state decompositions of different physical states. The wave function of an S-wave orthoquarkonia state $|\psi_Q\rangle$ is expanded as follows:

$$\begin{aligned}
|\psi_Q\rangle &= O(1)|Q\bar{Q}[{}^3S_1^{(1)}]\rangle + O(v)|Q\bar{Q}[{}^3P_J^{(8)}]g\rangle \\
&+ O(v^2)|Q\bar{Q}[{}^3S_1^{(1,8)}]gg\rangle + O(v^2)|Q\bar{Q}[{}^1S_0^{(8)}]g\rangle \\
&+ O(v^2)|Q\bar{Q}[{}^3D_J^{(1,8)}]gg\rangle + \dots
\end{aligned} \tag{4}$$

and the wave functions of a P-wave orthoquarkonium state $|\chi_{QJ}\rangle$ has a similar expansion:

$$\begin{aligned}
|\chi_{QJ}\rangle &= O(1)|Q\bar{Q}[{}^3P_J^{(1)}]\rangle + O(v)|Q\bar{Q}[{}^3S_1^{(8)}]g\rangle \\
&+ O(v^2)\dots
\end{aligned} \tag{5}$$

In the above equation (1,8) refers to singlet and octet state of the $Q\bar{Q}$ pair. After a $Q\bar{Q}$ is formed in its color octet state it may absorb a soft gluon and transform into $|\chi_{QJ}\rangle$ via eq. (5) and then become a J/ψ by photon decay. The $Q\bar{Q}$ pair in the color octet state can also emit two long wavelength gluons and become a J/ψ via eq. (4) and so on. The non-perturbative matrix elements can be fitted from other experiments or can be determined from lattice calculations.

In the color octet mechanism the p_T distribution differential cross section for J/ψ production is given by:

$$\begin{aligned}
\frac{d\sigma}{dp_T}(AB \rightarrow \psi_Q(\chi_J) + X) &= \sum_{a,b} \int dy \int dx_a x_a \\
&f_{a/A}(x_a, Q^2) x'_b f_{b/B}(x'_b, Q^2) \times \frac{2p_T}{x_a - \frac{M_T}{\sqrt{s}} e^y} \\
\frac{d\hat{\sigma}}{d\hat{t}}(ab \rightarrow C\bar{C}[{}^{2S+1}L_J^{(8)}]c \rightarrow \psi_Q(\chi_J)), &
\end{aligned} \tag{6}$$

where the partonic level differential cross section is given by

$$\begin{aligned}
\frac{d\hat{\sigma}}{d\hat{t}}(ab \rightarrow C\bar{C}[{}^{2S+1}L_J^{(8)}]c \rightarrow \psi_Q(\chi_J)) &= \frac{1}{16\pi\hat{s}^2} \\
\Sigma |\mathcal{A}(ab \rightarrow C\bar{C}[{}^{2S+1}L_J^{(8)}]c)_{\text{short}}|^2 &< 0 |\mathcal{O}_8^{\psi_Q(\chi_J)}({}^{2S+1}L_J)|0\rangle
\end{aligned} \tag{7}$$

In our calculation all the partonic level matrix elements squared

$$\Sigma |\mathcal{A}(ab \rightarrow C\bar{C}[{}^{2S+1}L_J^{(8)}]c)_{\text{short}}|^2$$

and the non-perturbative matrix elements

$$\langle 0 | \mathcal{O}_8^{\psi Q(\chi_J)} ({}^{2S+1}L_J) | 0 \rangle$$

are taken from [5].

For the rapidity distribution and total cross section of J/ψ production the leading contribution is proportional to α_s^2 and we will only consider that contribution here. In leading order, the parton fusion processes contribute to the total cross section for J/ψ (χ_J) production in pp collisions as follows:

$$\begin{aligned} \sigma^{pp \rightarrow J/\psi(\chi_J)} &= \Sigma_{a,b} \int dx_a \int dx_b f_{a/A}(x_a, Q^2) f_{b/B}(x_b, Q^2) \\ \sigma^{ab \rightarrow J/\psi(\chi_J)}(\hat{s}) &\delta(x_a x_b - 4m^2/s) \end{aligned} \quad (8)$$

where $\sigma^{ab \rightarrow J/\psi(\chi_J)}(\hat{s})$ is the partonic level cross section at leading order which are derived in [5, 11]. In the above equation m is the mass of the charm quark. At the leading order not all the processes contribute to the total cross section in the singlet and octet channel. In the color singlet channel the J/ψ production cross section at α_s^2 order is given by:

$$\sigma_1^{pp \rightarrow J/\psi}(s) = \sigma_1^{pp \rightarrow \chi_0}(s) BR_{\chi_0} + \sigma_1^{pp \rightarrow \chi_2}(s) BR_{\chi_2}. \quad (9)$$

Here BR_χ refers to the branching ratio of a χ to decay into a J/ψ . Similarly in the octet channel at the leading order the J/ψ production cross section is given by:

$$\begin{aligned} \sigma_8^{pp \rightarrow J/\psi}(s) &= \sigma_8^{pp \rightarrow J/\psi}(s) + \sigma_8^{pp \rightarrow \chi_1}(s) BR_{\chi_1} \\ &+ \sigma_8^{pp \rightarrow \chi_0}(s) BR_{\chi_0} + \sigma_8^{pp \rightarrow \chi_2}(s) BR_{\chi_2}. \end{aligned} \quad (10)$$

In the above equations the direct J/ψ production and the decay of χ_c with their corresponding branching ratios to J/ψ are included. In the leading order we use the same values of the non-perturbative matrix elements used in the singlet and octet channels as in [12].

We will use the GRV98[13] and MRST99 [14] parton distribution functions inside the proton. The factorization scales are set to be $Q = 2m$ for the total cross section and rapidity distribution plots, and $Q = \sqrt{p_T^2 + M^2}$ for the plot of the p_T distribution.

In Fig.1 we present the p_T distribution of the J/ψ production cross section separately for the color singlet and color octet mechanism including the effects of cuts due to the PHENIX detector acceptance range. We have considered all the parton fusion processes [5, 15] in our calculation. In these plots we have used the GRV98 and MRST99 parton

distribution functions. As the non-perturbative NRQCD matrix elements has uncertainties as given in [5] we present two plots for each of the PDF's which correspond to the upper and lower limit on the non-perturbative matrix elements. The solid line corresponds to the results obtained by using the GRV98 PDF's with lowest values of the non-perturbative matrix elements as given in [5]. The upper dashed line corresponds to the results obtained by using the GRV98 PDF's with highest values of the non-perturbative matrix elements. The upper dot-dashed line corresponds to the results obtained by using the MRST99 PDF's with highest values of the non-perturbative matrix elements. The lower dot-dashed line corresponds to the results obtained by using the MRST99 PDF's with lowest values of the non-perturbative matrix elements. The lower dashed line corresponds to the color singlet contribution. We have compared our calculation with the recent PHENIX data (run3). The daggers are recent PHENIX data taken from [8]. It can be seen from the figure that the color singlet contribution is more than an order of magnitude smaller than the octet contribution. On the other hand, the color octet mechanism with only parton fusion processes reproduces the recent PHENIX data very well. Thus for $p_T \leq 5\text{GeV}$ we do not find it necessary to include contributions from the parton fragmentation processes. We have not compared our calculation with the data below p_T equals to 2 GeV as pQCD calculations are not valid at such low transverse momenta. In the near future PHENIX will have sensitivity up to $p_T = 10\text{GeV}$. This new data will allow us to decide whether fragmentation processes contributions within color octet mechanism are important at higher p_T and whether their inclusion will allow us to understand the data.

In Fig. 2 we present the rapidity distribution of the J/ψ production cross section in pp collisions at RHIC at $\sqrt{s} = 200$ GeV. We have taken the charm quark mass equal to 1.45 GeV in our calculation. The solid line is the results obtained by using the GRV98 PDF's with lowest values of the non-perturbative matrix elements. The upper dashed line corresponds to the results obtained by using the GRV98 PDF's with highest values of the non-perturbative matrix elements. The upper dot-dashed line corresponds to the results obtained by using the MRST99 PDF's with highest values of the non-perturbative matrix elements. The lower dot-dashed line corresponds to the results obtained by using the MRST99 PDF's with lowest values of the non-perturbative matrix elements. The PHENIX experimental data [8] are shown in the figure as daggers. The rapidity range covered by PHENIX at RHIC is from $-3 < y < 3$. The color singlet contribution is also shown as the lower dashed line (here

we only show the results using the GRV98 PDF's) which is very small when compared with the color octet contribution. It can be seen that just including the color octet contribution explains the run3 PHENIX data.

Finally, we present the total cross section for J/ψ production in pp collisions at $\sqrt{s} = 200$ GeV at RHIC and compare it with the run3 PHENIX data. In the color octet case we find $B\sigma_{J/\psi} = 159 \pm 6$ (nb) which is in very good agreement with the PHENIX collaboration experimental value which is reported as 159 (nb) [8]. The ± 6 (nb) is due to the errors in the non-perturbative matrix elements as given in [5]. In the above total cross section computation we have used charm quark mass equal to 1.45 GeV and the MRST99 parton distribution function inside the proton. The agreement of color octet mechanism predictions with the PHENIX experimental data is remarkable in all aspects, *i.e.* in p_T distribution, in rapidity distribution and in total cross section measurements at $\sqrt{s} = 200$ GeV pp collisions.

Before summarizing, we briefly discuss the uncertainties due to PDF's, non-perturbative matrix elements etc. As can be seen from Fig. 1 and Fig. 2 that both GRV98 and MRST99 PDF's describe the data very well. We have also checked that the recent CTEQ6M PDF's also explain the data very well. The uncertainty in the results due to the errors in the non-perturbative matrix elements are given in Fig. 1 and 2 and also in the total cross section.

In summary, in this letter, we have studied J/ψ production in pp collisions at RHIC at $\sqrt{s} = 200$ GeV within the PHENIX detector acceptance range by using the color singlet and the color octet mechanism within pQCD and NRQCD and have compared them with the recent PHENIX experimental data. We have demonstrated that the color octet mechanism using only parton fusion processes is able to reproduce the RHIC data on the p_T distribution, rapidity distribution and total cross section of J/ψ production. This is done without any normalization factor modifications and using matrix elements extracted from the Tevatron and other experiments. The color singlet mechanism gives negligible contributions when compared to the octet contributions at this energy. Our results confirm the applicability of the color octet mechanism found at the Tevatron.

It is important to identify the correct mechanism for J/ψ production in pp collisions at RHIC if we want to study J/ψ suppression as a signature of quark-gluon plasma detection in AuAu collisions at $\sqrt{s} = 200$ GeV [7]. It is also important if we hope to extract the polarized gluon distribution function from the data on polarized pp collisions at RHIC. The latter will

be important for isolating interference terms which can be used to explore various models which predict non standard model TeV physics.

Acknowledgements: We thank Rajiv Gai, Sourendu Gupta, Pat McGaughey, Jack Smith and George Sterman for useful discussions. This work was supported in part by the National Science Foundation grant PHY-0098527 and Department of Energy, under contract W-7405-ENG-36.

* Electronic address: fcooper@nsf.gov

† Electronic address: mliu@lanl.gov

‡ Electronic address: nayak@insti.physics.sunysb.edu

- [1] E. L. Berger and D. Jones, Phys. Rev. D23 (1981) 1521; R. Baier and R. Ruckl, Z. Phys. C19 (1983) 251.
- [2] For earlier works on J/ψ production; see for example; S. D. Ellis, M. Einhorn and C. Quigg; Phys. Rev. Lett. 36 (1976) 1263.
- [3] G. T. Bodwin, E. Braaten and G. P. Lepage, Phys. Rev. D51 (1995) 1125; 55 (1997) 5855; E. Braaten, M. A. Doncheski, S. Fleming, and M. Mangano, Phys. Lett. B333 (1994) 548; D. P. Roy and K. Sridhar, Phys. Lett. B339 (1994) 141; M. Cacciari and M. Greco, Phys. Rev. Lett. 73 (1994) 1586; G. T. Bodwin, E. Braaten and G. P. Lepage, Phys. Rev. D46 (1992), R1914; E. Braaten and S. Fleming, Phys. Rev. Lett. 74 (1995) 3327; S. Gupta and K. Sridhar, Phys. Rev. D54 (1996) 5545; 55 (1997) 2650; M. Cacciari and M. Kramer, Phys. Rev. Lett. 76 (1996) 4128; M. Beneke and I. Rothstein, Phys. Rev. D54 (1996) 434; M. Klasen, B. A. Kniehl, L. N. Mihaila and M. Steinhauser; Phys. Rev. D68 (2003) 034017.
- [4] E. Braaten, S. Fleming and T. C. Yuan, Ann. Rev. Nucl. Part. Sci. 46 (1996) 197, hep-ph/9602374 and references therein.
- [5] P. Cho and A. K. Leibovich, Phys. Rev. D53 (1996) 6203.
- [6] CDF Collaboration, F. Abe *al.*, Phys. Rev. Lett. 75 (1995) 4358; CDF Collaboration, Report No. Fermilab-Conf-94/136-E, 1994, Fermilab-Conf-95/128-E, 1995;
- [7] T. Matsui and H. Satz, Phys. Lett. B178 (1986) 416; X-M. Xu *et al.*, Phys. Rev. C53 (1996) 3051; G. C. Nayak, JHEP 9802 (1998) 005; G. C. Nayak, Phys. Lett. B442 (1998) 427; F. Cooper, E. Mottola and G. C. Nayak, Phys. Lett. B555 (2003) 181; G. C. Nayak, A. Dumitru,

- L. McLerran and W. Greiner, Nucl. Phys. A687 (2001) 457; G. C. Nayak and R. S. Bhalerao, Phys. Rev. C61 (2000) 054907.
- [8] R. G. De Cassagnac, For PHENIX Collaboration, Quark Matter 2004, Oakland, California, January 12-17, 2004.
- [9] E. J. Eichten and C. Quigg, Phys. Rev. D52 (1995) 1726.
- [10] G. T. Bodwin, E. Braaten and G. P. Lepage, Phys. Rev. D46 (1992) 1914.
- [11] S. Fleming and I. Kaksymyk Phys.Rev.D54:3608-3618,1996.
- [12] M. Beneke, I. Z. Rothstein, Phys. Rev. D54 (1996) 2005.
- [13] M. Glueck, E. Reya and A. Vogt, Euro. Phys. J. C5 (1998) 461.
- [14] A. D. Martin, R. G. Roberts, W. J. Stirling and R. S. Thorne, Eur. Phys. J.C23 (2002) 73.
- [15] G. C. Nayak, M. X. Liu and F. Cooper, Phys. Rev. D68 (2003) 034003.

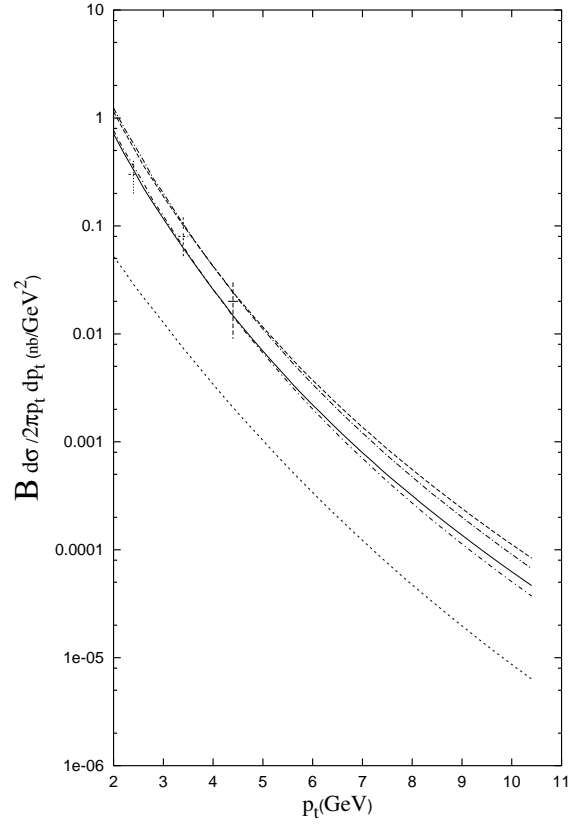


FIG. 1: p_T distribution of J/ψ production cross section in pp collisions at $\sqrt{s} = 200$ GeV at RHIC in the PHENIX detector acceptance range. The solid and upper dashed lines and upper/lower dot-dashed lines correspond to color octet mechanism predictions with GRV98 and MRST99 PDF's. The lower dashed line is the color singlet contribution. The daggers are run3 PHENIX experimental data.

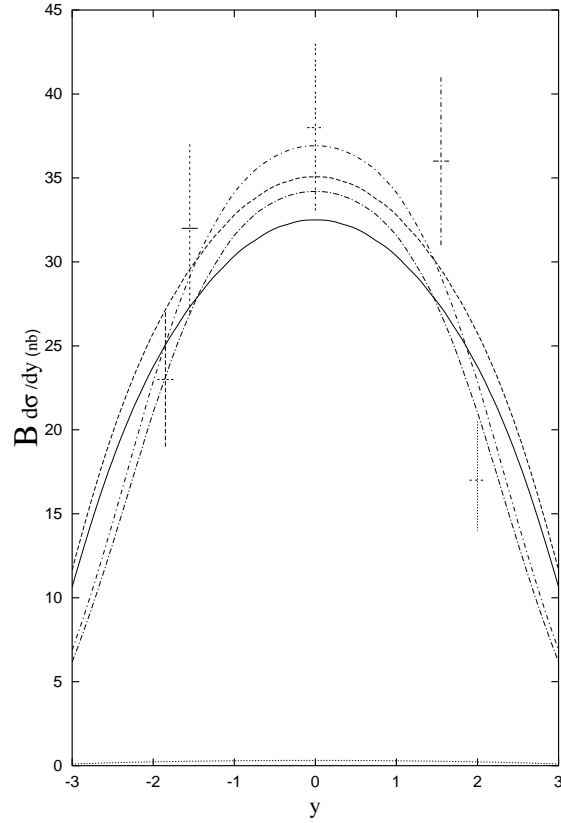


FIG. 2: Rapidity distribution of J/ψ production cross section in pp collisions at $\sqrt{s} = 200$ GeV at RHIC in the PHENIX detector acceptance range. The solid and upper dashed lines and upper/lower dot-dashed lines correspond to color octet mechanism predictions with GRV98 and MRST99 PDF's. The lower dashed line is the color singlet contribution. The daggers are run3 PHENIX experimental data.